

# Magnetic vortex as a ground state for micron-scale antiferromagnetic samples

E. G. Galkina,<sup>1,2</sup> A. Yu. Galkin,<sup>3</sup> B. A. Ivanov,<sup>4,2,\*</sup> and Franco Nori<sup>2,5</sup>

<sup>1</sup>*Institute of Physics, 03028 Kiev, Ukraine*

<sup>2</sup>*RIKEN Advanced Science Institute,  
Wako-shi, Saitama, 351-0198, Japan*

<sup>3</sup>*Institute of Metal Physics, 03142 Kiev, Ukraine*

<sup>4</sup>*Institute of Magnetism, 03142, Kiev, Ukraine*

<sup>5</sup>*Department of Physics, The University of Michigan, Ann Arbor, MI 48109-1040, USA,*

(Dated: October 30, 2018)

## Abstract

Here we consider micron-sized samples with any axisymmetric body shape and made with a canted antiferromagnet, like hematite or iron borate. We find that its ground state can be a magnetic vortex with a topologically non-trivial distribution of the sublattice magnetization  $\vec{l}$  and planar coreless vortex-like structure for the net magnetization  $\vec{M}$ . For antiferromagnetic samples in the vortex state, in addition to low-frequency modes, we find high-frequency modes with frequencies over the range of hundreds of gigahertz, including a mode localized in a region of radius  $\sim 30$ – $40$  nm near the vortex core.

PACS numbers: 75.50.Ee, 76.50.+g, 75.30.Ds, 75.10.Hk

## I. INTRODUCTION

The magnetic properties of submicron ferromagnetic samples shaped as circular cylinders (magnetic dots) are attracting considerable attention mainly due to their potential applications (see, e.g., Ref. 1). Circular dots possess an equilibrium magnetic configuration which corresponds to a vortex structure just above the single domain length scale, with radius  $R > R_{\text{crit}} \sim 100\text{--}200$  nm. The ferromagnetic vortex state consists of an in-plane flux-closure magnetization distribution and a central core with radius  $\sim 20\text{--}30$  nm, magnetized perpendicular to the dot plane. Reducing the magnetostatic energy comes at the cost of a large exchange energy near the vortex core, as well as the magnetostatic energy caused by the core magnetization. Due to spatial quantization, the magnon modes for dots have a discrete spectrum. The possibility to control the localization and interference of magnons spawned *magnonics*, trying to use these modes for developing a new generation of microwave devices with submicron active elements (see, e.g., Ref. 2).

These samples also provide an ideal experimental system for studying static and especially dynamic properties of relatively simple topologically non-trivial magnetic structures which are fundamentally interesting objects in different research areas of physics. The investigation of the non-uniform states of ordered media with non-trivial topology of the order parameter can be considered as one of the most impressive achievements of modern condensed matter physics (see, e.g., Ref. 3), and field theory (see, e.g., Ref. 4). For example, vortices (topological solitons) appear in many systems with continuously degenerate ground states, whose properties are determined by some phase-like variable  $\phi$ , including superconductors (see, e.g., Ref. 5), quantum liquids (helium-II, and different phases of superfluid  $^3\text{He}$ , see, e.g., Ref. 3), dilute Bose-Einstein condensates,<sup>6</sup> and also different models of magnets: ferromagnets and antiferromagnets,<sup>7–9</sup> and spin nematics.<sup>10,11</sup> The contribution of topological excitations (vortices and vortex pairs) to the thermodynamics and response functions of a two-dimensional ordered media are well known. At low temperatures, vortices are bound into pairs, forming a Berezinskii phase with absence of long-range order, but with quasi-long-range order. The unbinding of the vortex pairs at high enough temperatures,  $T > T_{\text{BKT}}$ , leads to the Berezinskii-Kosterlitz-Thouless phase transition. In particular, the translational motion of vortices leads to a central peak in the dynamic correlation functions, which has been observed experimentally; see Refs. 9,12,13 and references therein.

Physical systems with a topological defect as a ground state are of special interest. The role of vortices in rotating superfluid systems is known.<sup>3</sup> Additional examples include single-connected samples of the A-phase of superfluid  $^3\text{He}$ , where the true energy minimum is a non-trivial state (bujoom) with a surface vortex-like singularity.<sup>3</sup> Moreover, non-uniform states can also appear in small magnetic samples having high enough surface anisotropy.<sup>14,15</sup> Among these examples, magnets are interesting because samples bearing vortices can be prepared of micrometer and sub-micrometer size, and vortices can be present at high enough temperatures, including room temperature. Furthermore, their static and dynamic properties can be observed using different techniques.(e.g., Refs. 1,16,17)

### A. Summary of results

All previous studies of magnetic vortices caused by magnetic dipole interactions were carried out on magnetic samples made with soft ferromagnets with large magnetization  $M_s$ , like permalloy, with  $4\pi M_s \sim 1$  T. In this work, we show that vortices can be a ground state for micron-scale samples with axial symmetry, but now made with another important class of magnetic materials: antiferromagnets with easy-plane anisotropy and Dzyaloshinskii–Moriya interaction (DMI). Some antiferromagnets possess a small, but non-zero, net magnetization caused by a weak non-collinearity of the sublattices (sublattice canting) originated from the DMI. As we show here, the formation of a vortex in an AFM sample leads to a more effective minimization of the non-local magnetic dipole interaction, compared to the case with ferromagnetic dots. Typical antiferromagnets include hematite  $\alpha\text{-Fe}_2\text{O}_3$ , iron borate  $\text{FeBO}_3$ , and orthoferrites.<sup>7</sup> These materials exhibit magnetic ordering at high temperatures. Moreover, they have unique physical properties: orthoferrites and iron borate are transparent in the optical range and have a strong Faraday effect, and the magnetoelastic coupling is quite high in hematite and iron borate.<sup>7</sup> For antiferromagnets, typical frequencies of spin oscillations have values in a wide region, from gigahertz to terahertz, which can be excited by different techniques (not only the standard one using of ac-magnetic fields, but with optical or acoustic methods as well). Spin oscillations can also be triggered by ultra-short laser pulses.<sup>18–21</sup> For antiferromagnetic (AFM) samples in the vortex state, here we derive a rich spectrum of discrete magnon modes with frequencies from sub-gigahertz to hundreds of gigahertz, including a mode localized near the vortex core. These results should help to

extend the frequency range of magnonic microwave devices till sub-terahertz region.

## II. MODEL

For antiferromagnets, the exchange interaction between neighboring spins facilitates an antiparallel spin orientation, which leads to a structure with two antiparallel magnetic sublattices,  $\vec{M}_1$  and  $\vec{M}_2$ ,  $|\vec{M}_1| = |\vec{M}_2| = M_0$ . To describe the structure of this antiferromagnet, it is convenient to introduce irreducible combinations of the vectors  $\vec{M}_1$  and  $\vec{M}_2$ , the net magnetization  $\vec{M} = \vec{M}_1 + \vec{M}_2 = 2M_0\vec{m}$ , and the sublattice magnetization vector  $\vec{l} = (\vec{M}_1 - \vec{M}_2)/2M_0$ . The vectors  $\vec{m}$  and  $\vec{l}$  are subject to the constraints:  $(\vec{m} \cdot \vec{l}) = 0$  and  $\vec{m}^2 + \vec{l}^2 = 1$ . As  $|\vec{m}| \ll 1$ , the vector  $\vec{l}$  could be considered as a unit vector. The mutual orientation of the sublattices is determined by the sum of the energy of uniform exchange  $W_{\text{ex}}$  and the DMI energy,  $W_{\text{DM}}$ ,

$$W_{\text{ex}} = H_{\text{ex}}M_0\vec{m}^2, \quad W_{\text{DM}} = 2M_0H_{\text{D}}[\vec{d} \cdot (\vec{m} \times \vec{l})],$$

where the unit vector  $\vec{d}$  is directed along the symmetry axis of the magnet. Here we will not discuss the role of external magnetic fields. The parameters  $H_{\text{ex}} \sim 3 \cdot 10^2 - 10^3$  T and  $H_{\text{D}} \sim 10$  T are the exchange field and DMI field, respectively. Using the energy ( $W_{\text{ex}} + W_{\text{DM}}$ ) and the dynamical equations for  $\vec{M}_1$  and  $\vec{M}_2$ , one can find,<sup>7</sup>

$$\vec{M} = M_{\text{DM}} \left( \vec{d} \times \vec{l} \right) + \frac{2M_0}{\gamma H_{\text{ex}}} \left( \vec{l} \times \frac{\partial \vec{l}}{\partial t} \right), \quad M_{\text{DM}} = \frac{2H_{\text{D}}M_0}{H_{\text{ex}}}, \quad (1)$$

where  $\gamma$  is the gyromagnetic ratio. The first term gives the static value of the antiferromagnet net magnetization  $M_{\text{DM}}$ , comprising a small parameter,  $H_{\text{D}}/H_{\text{ex}} \sim 10^{-2}$ , and the second term describes the dynamic canting of sublattices; see Ref. 7 for details. Note that  $M_{\text{DM}}$  is much smaller than either  $M_0$  or the value of  $M_s$  for typical ferromagnets. However, the role of the magnetostatic energy caused by  $M_{\text{DM}}$  could be essential, and could lead to the appearance of a domain structure for antiferromagnets,<sup>7,22</sup> and the magnetic dipolar stabilization of the long-range magnetic order for the 2D case.<sup>23</sup> We will show that for the formation of equilibrium vortices, antiferromagnets have some advantages compared with soft ferromagnets.

The static and especially dynamic properties of antiferromagnets are essentially different from the ones of ferromagnets. The spin dynamics of an antiferromagnet can be described using the so-called sigma-model ( $\sigma$ -model), a dynamical equation only for the vector  $\vec{l}$  (see,

e.g., Ref. 7). In this approach, the magnetization  $\vec{M} = \vec{M}_1 + \vec{M}_2 = 2M_0\vec{m}$  is a slave variable and can be written in terms of the vector  $\vec{l}$  and its time derivative, see Eq. (1). Within the  $\sigma$ -model, the equation for the normalized (unit) antiferromagnetic vector  $\vec{l} = \vec{L}/|\vec{L}|$  can be written through the variation of the Lagrangian  $\mathcal{L}[\vec{l}]$

$$\mathcal{L} = \frac{A}{2c^2} \int \left( \frac{\partial \vec{l}}{\partial t} \right)^2 d^3x - W[\vec{l}], \quad (2)$$

where  $A$  is the non-uniform exchange constant,  $c = \gamma\sqrt{AH_{\text{ex}}/M_0}$  is the characteristic speed describing the AFM spin dynamics,  $W[\vec{l}]$  is the functional describing the static energy of the AFM. It is convenient to present the energy functional in the form  $W[\vec{l}] = W_0[\vec{l}] + W_m$ ,

$$\begin{aligned} W_0[\vec{l}] &= \frac{1}{2} \int [A(\nabla\vec{l})^2 + K \cdot l_z^2] d^3x, \\ W_m &= -\frac{1}{2} \int \vec{M}\vec{H}_m d^3x, \end{aligned} \quad (3)$$

where the first term  $W_0[\vec{l}]$  determines the local model of an AFM, including the energy of non-uniform exchange and the easy-plane anisotropy energy through only the vector  $\vec{l}$ ,  $K > 0$  is the anisotropy constant, and the  $xy$ -plane is the easy plane for spins. The second (non-local) term  $W_m$  is the magnetic dipole energy,  $\vec{H}_m$  is the demagnetization field caused by the AFM magnetization (1), the field  $\vec{H}_m$  is determined by the magnetostatic equation,

$$\text{div}(\vec{H}_m + 4\pi\vec{M}) = 0, \quad \text{curl}\vec{H}_m = 0,$$

$\vec{M} = 2M_0\vec{m}$ , with the standard boundary conditions: the continuity of the normal component of  $(\vec{H}_m + 4\pi\vec{M})$  and the tangential component of  $\vec{H}_m$ , on the border of the sample. Thus, sources of  $\vec{H}_m$  can be considered as formal ‘‘magnetic charges’’, where volume charges equal to  $\text{div}\vec{M}$  and surface charges equal  $-\vec{M} \cdot \vec{n}$ , where  $\vec{n}$  is the unit vector normal to the border ( see the monographs 22, 24 for general considerations and Refs. 25,26 for application to vortices). As mentioned above, the presence of surface anisotropy with the constant  $K_{\text{surf}}$  can contribute to the energy of a micron-scale sample leading to non-uniform states.<sup>14,15</sup> But this contribution is essential for a high enough anisotropy  $K_{\text{surf}} \gg K$  and quite small samples, and we will neglect this contribution, and concentrate on an alternative source of non-uniform states, namely, the magnetic dipole interaction.

### A. Dynamic sigma-model

The variation of the total Lagrangian (2) gives a dynamic  $\sigma$ -model equation, where the static spin distribution for an uniaxial antiferromagnet is determined by the minimization of an energy functional of the form of Eq. (3). It is useful to start with a variation of the local energy  $W_0[\vec{l}]$  only, that gives a general two-dimensional (2D) vortex solution for the vectors  $\vec{l}$ ,  $\vec{M}$  of the form

$$\begin{aligned}\vec{l} &= \vec{e}_z \cos \theta + \sin \theta [\vec{e}_x \cos(\chi + \varphi_0) + \vec{e}_y \sin(\chi + \varphi_0)], \\ \vec{M} &= M_{\text{DM}} \cdot \sin \theta [\vec{e}_y \cos(\chi + \varphi_0) - \vec{e}_x \sin(\chi + \varphi_0)],\end{aligned}\quad (4)$$

where  $\theta = \theta(r)$ ,  $r$  and  $\chi$  are polar coordinates in an easy-plane of the magnet, the vector  $\vec{e}_z$  is the hard axis, and the value of  $\varphi_0$  is arbitrary. The function  $\theta(r)$  is determined by the ordinary differential equation

$$\frac{d^2\theta}{dx^2} + \frac{1}{x} \frac{d\theta}{dx} = \sin \theta \cos \theta \left( \frac{1}{x^2} - 1 \right), \quad x = \frac{r}{l_0}, \quad (5)$$

and exponentially tends to  $\pi/2$  for  $r \gg l_0$ , with characteristic size  $l_0 = \sqrt{A/K}$ . Also, in the center of the vortex (at  $r = 0$ ), the value of  $\sin \theta(r = 0) = 0$ , see Fig. 1.

In the region of the vortex core,  $\vec{l}$  deviates from the easy-plane, and the anisotropy energy increases. The state (4) is non-uniform, increasing the exchange energy. Therefore, for the local easy-plane model, the appearance of a vortex costs some energy, i.e., the vortex corresponds to excited states of antiferromagnets. Also, vortex excitations are important for describing of thermodynamics of 2D antiferromagnets.<sup>27</sup> As we will show in the next section, considering the dipolar energy  $W_m[\vec{l}]$ , a vortex can be the ground state of a circular magnetic sample made with canted antiferromagnets.

### III. ENERGY OF THE VORTEX AND UNIFORM STATES

For small samples made with canted antiferromagnets, the energy loss caused by a vortex within the local model  $W = W_0[\vec{l}]$  can be compensated by the energy of the magnetic dipole interaction. To explain this, note that for a uniform distribution state, the contribution  $W_m$  unavoidably results in a loss of the system energy, which is proportional to the volume  $V$  of the sample.<sup>22,24</sup> The energy of the uniform state could be estimated as

$$E^{(\text{homog})} = 2\pi N M_{\text{DM}}^2 V = 2\pi N M_0^2 (2H_{\text{D}}/H_e)^2 V, \quad (6)$$

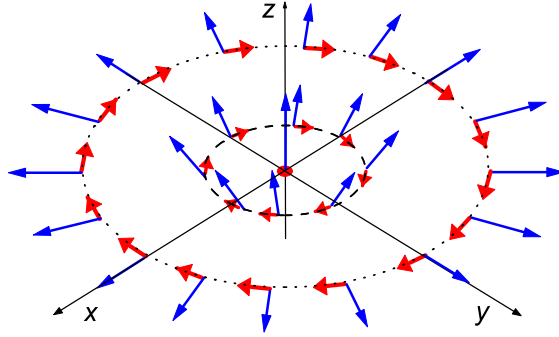


FIG. 1: (Color online) Schematic structure of the AFM vortex for  $\cos \theta(r=0) = 1$  and the special value of the arbitrary parameter  $\varphi_0 = 0$ . The vectors  $\vec{l}$  (thin blue arrows in the radial direction) and  $\vec{M}$  (thick tangential red arrows; shown not in scale) are depicted for the area of the core (dashed circle) and far from it (larger dotted circle). The red dot at the origin indicates the value  $\vec{M} = 0$  for the state with  $\vec{l} = \vec{e}_z$  perpendicular to the plane.

where  $N$  is the effective demagnetizing factor in the direction perpendicular to the sample axis.<sup>22,24</sup>

For magnetic samples other than an ellipsoid (for example, for a cylinder with a finite aspect ratio  $R/L$ ), the distribution of the field  $\vec{H}_m$  is non-uniform, leading to a non-topological quasi-uniform state known as a flower state.<sup>28</sup> But a detailed numerical analysis shows,<sup>29–32</sup> in all the stability region of the quasi-uniform state where Eq. (6) is valid, the corresponding value of  $N$  is practically the same as for the uniform magnetization, and the numerical results<sup>29–32</sup> obtained within this approximation are in good agreement with experiments.<sup>28</sup>

For the static vortex state (4) with a chosen value of  $\sin \varphi_0 = 0$ , with  $\vec{M} \propto (\vec{d} \times \vec{l})$ , one can find

$$\vec{M} = \sigma M_{\text{DM}} \cdot \sin \theta (-\vec{e}_x \sin \chi + \vec{e}_y \cos \chi), \quad (7)$$

where  $\sigma = \cos \varphi_0 = \pm 1$ . A unique property of the state (7) is that it can also *exactly* minimize the energy of the magnetic dipole interaction  $W_m$ , giving  $\vec{H}_m = 0$  in the overall space. Indeed, the projection of  $\vec{M}$  on the lateral surface of any axisymmetric body with its symmetry axis parallel to the  $z$ -axis equals to zero. Also  $\text{div} \vec{M} = 0$  for the distribution given by Eq. (7). Moreover, due to the symmetry of the DMI,  $(\vec{M} \cdot \vec{d}) = 0$ , the distribution of the magnetization  $\vec{M}$  (7) is *purely planar* (in contrast to  $\vec{l}$ ) and the out-of-plane component of  $\vec{M}$  is absent. In the vicinity of the vortex core, the length of the vector  $\vec{M}$  decreases, turning

to zero in the vortex center, see Fig. 1. Such feature is well known for domain walls in some orthoferrites.<sup>7</sup> Thus, the AFM vortex is the unique spin configuration which does not create a demagnetization field in a singly-connected body (for ferromagnet with  $|\vec{M}| = \text{const}$ , a configuration with  $\vec{H}_m \equiv 0$  can be possible only for magnetic rings having the topology of a torus).

### A. Comparing the energies of the vortex and uniform states for antiferromagnets

Let us now compare the energies of the vortex state and the uniform state for AFM samples shaped as a cylinder with height  $L$  and radius  $R$ . For the vortex state,  $\vec{H}_m = 0$  over the the sample volume, and the vortex energy is determined by the simple formula,<sup>7</sup>

$$E_v = \pi AL \ln \left( \rho \frac{R}{l_0} \right), \quad (8)$$

where  $\rho \approx 4.1$  is a numerical factor. For long cylinders with  $L \gg R$ , the value of  $N \simeq 1/2$  and the vortex state becomes favorable if the radius  $R$  exceeds some critical value  $R_{\text{crit}}$ ,

$$R \geq R_{\text{crit}} = 2l_{\text{dip}} \sqrt{\ln \left( \frac{l_{\text{dip}}}{l_0} \right)},$$

$$l_{\text{dip}} = \sqrt{\frac{A}{4\pi M_{\text{DM}}^2}}, \quad (9)$$

where  $l_{\text{dip}}$  determines the spatial scale corresponding to the magnetic dipole interaction. Note that  $l_{\text{dip}}$  comprises a large parameter  $H_e/H_D \sim 30\text{--}100$ , and  $l_{\text{dip}} \gg l_0$ . In the case of a thin disk,  $L \ll R$  and the demagnetization field energy becomes<sup>25,26</sup>

$$E^{(\text{homog})} = 2\pi RL^2 M_{\text{DM}}^2 \ln(4R/L),$$

and the vortex state is energetically favorable for  $RL \geq (RL)_{\text{crit}} = 2l_{\text{dip}}^2$ .

For concrete estimates we take the parameters of iron borate,  $A = 0.7 \cdot 10^{-6}$  erg/cm,  $K = 4.9 \cdot 10^6$  erg/cm<sup>3</sup> and  $4\pi M_{\text{DM}} = 120$  Oe. Then we obtain that  $l_0 = 3.8$  nm, i.e., the core size is of the same order of magnitude as for a typical ferromagnet (for permalloy  $l_0 = 4.8$  nm). The value  $l_{\text{dip}}$  is essentially higher, e.g., for iron borate  $l_{\text{dip}} = 220$  nm. Combining these data one finds for the long cylinder  $R_{\text{crit}} = 0.9 \mu\text{m}$ . For a thin disk sample the characteristic scale has submicron value:  $\sqrt{(RL)_{\text{crit}}} = 0.4 \mu\text{m}$ . Similar estimates are obtained for orthoferrites, and somewhat higher values for hematite. Thus, despite the fact



that the characteristic values for the dipole length  $l_{\text{dip}}$  for a ferromagnet and antiferromagnet differ hundredfold, the characteristic critical sizes differ not so drastically (for permalloy  $R_{\text{crit}} \sim 100\text{-}200$  nm). This is caused by the aforementioned fact that the magnetic field created by the vortex core is completely absent for the AFM vortex. The situation here is common to that for ferromagnetic nanorings, where the vortex core is absent. Despite the fact that the vortex core size in ferromagnetic dots is rather small, the core contribution to  $W_m$  for ferromagnetic dots of rather big radius  $R \geq 0.5 \mu\text{m}$  is negligible, but it becomes essential for small samples with  $R$  close to the critical size. Note as well that the vortex core magnetic field in the ferromagnet destroys the purely 2D character of the distribution of  $\vec{M}$  in Eq. (4), and the core size changes over the thickness of the sample. For an AFM vortex, the value of  $\vec{H}_m$  equals exactly zero, and a truly 2D distribution of  $\vec{l}$  and  $\vec{M}$ , independent of the coordinate  $z$  along the body axis, is possible.

#### IV. MAGNON MODES FOR VORTEX STATE ANTIFERROMAGNETIC SAMPLES

The dynamics of  $\vec{l}$  considered within the  $\sigma$ -model approach differs from the dynamics of a ferromagnetic magnetization described by the Landau–Lifshitz equation. The main difference is that the  $\sigma$ -model equation contains a dynamical term with a second-order time derivative of  $\vec{l}$ , whereas the Landau–Lifshitz equation is first-order in time. For this reason, for antiferromagnets, two magnon branches exist, instead of one for ferromagnets.<sup>7</sup> For both AFM modes, the elliptic polarization of the oscillations of  $\vec{M}_1$  and  $\vec{M}_2$  is such that the oscillations of the vector  $\vec{l}$  have a linear polarization.<sup>7</sup> For an easy-plane antiferromagnet, these two branches are a low-frequency quasi-ferromagnetic (QFM) branch and a high-frequency quasi-antiferromagnetic (QAF) branch, respectively. QFM magnons involve oscillations of the vectors  $\vec{l}$  and  $\vec{M}$  in the easy-plane, with a weak deviation of  $\vec{M}$  from the easy-plane caused by the last term in (1). The second QAF branch corresponds to the out-of-plane oscillations of  $\vec{l}$  with the dispersion law

$$\omega_{\text{QAF}}(\vec{k}) = \sqrt{\omega_{\text{g}}^2 + c^2 \vec{k}^2}, \quad \omega_{\text{g}} = \gamma \sqrt{2H_{\text{ex}} H_{\text{a}}},$$

where  $\vec{k}$  is the magnon wave vector. The gap of the QAF branch,  $\omega_{\text{g}}$ , contains a large value  $H_{\text{ex}}$  and attains hundreds of GHz. Thus compared to ferromagnets, both the magnon

frequency and speed for AFM dynamics contain a large parameter

$$\sqrt{H_{\text{ex}}/H_{\text{a}}} \sim 30-100,$$

( $H_{\text{ex}}$  and  $H_{\text{a}}$  are the exchange field and the anisotropy field, respectively) which can be referred as the *exchange amplification* of the dynamical parameters of AFM. The frequency  $\omega_{\text{g}}$  of AFM magnon modes reaches hundreds of GHz, with values  $\sim 170$  GHz for hematite, 100-500 GHz for different orthoferrites, and 310 GHz for iron borate.<sup>33</sup> Recent studies using ultra-short laser pulses showed the possibility to excite spin oscillations of non-small amplitude for orthoferrites<sup>18,19</sup> and iron borate.<sup>20</sup> This technique can be also extended to other antiferromagnets, including those without Dzyaloshinskii-Moriya interaction.<sup>21</sup>

Since the magnon spectra of bulk ferromagnets and antiferromagnets differ significantly, one can expect an essential difference for the magnon modes of the vortex state for both AFM and ferromagnetic samples. Let us briefly recall the properties of normal modes for disk-shaped vortex state ferromagnetic samples (ferromagnetic dots). For such dots, the presence of a discrete spectrum of magnon modes, characterized by the principal number (the number of nodes)  $n$  and the azimuthal number  $m$ , is well established.<sup>34-37</sup> This spectrum includes a single low-frequency mode of precessional motion of a vortex core ( $n = 0$ ,  $m = 1$ ) with a resonant frequency in the subGHz region,<sup>38</sup> a set of radially symmetrical modes with  $m = 0$ ,<sup>39</sup> and also a system of slightly splinted doublets with azimuthal numbers  $m = \pm|m|$ , with frequencies  $\omega_{|m|,n} \neq \omega_{-|m|,n}$ , and  $\omega_{|m|,n} - \omega_{-|m|,n} \ll \omega_{|m|,n}$ ; see Refs. 25,26,40. The same classification is valid for vortices for local easy-plane ferromagnets.<sup>41</sup> Wysin<sup>42</sup> demonstrated the direct correspondence of the gyroscopic character of vortex dynamics and doublet splinting.

For an AFM in the vortex state, small sample each of two magnon branches, QFM and QAF, produce a set of discrete modes with given  $n$  and  $m$ ; however, their properties are different compared to that of a ferromagnetic dot. Below we present a general analysis of small oscillations above the vortex ground state.

### A. General equations and mode symmetry.

The dynamics of small deviations from the AFM static vortex solution will be considered here for a thin circular sample (AFM dot) only, where the  $z$ -dependence of the vectors  $\vec{l}$

and  $\vec{m}$  can be neglected. It is convenient to introduce a local set of orthogonal unit vectors  $\vec{e}_1$ ,  $\vec{e}_2$  and  $\vec{e}_3$ , where  $\vec{e}_3$  coincides with the local direction of the unit vector  $\vec{l}$  in the vortex,  $\vec{e}_3 = \vec{l}(x, y) = \cos \theta_0 \vec{e}_z + \sin \theta_0 \hat{r}$ , see Fig. 1,  $\vec{e}_2 = -\vec{e}_x \sin \chi + \vec{e}_y \cos \chi = \hat{\chi}$ , and  $\vec{e}_1 = (\vec{e}_2 \times \vec{e}_3)$ . It is easy to see that the projection  $(\vec{l} \cdot \vec{e}_1) = \vartheta$  describes small deviations of  $\theta$  from the vortex ground state,  $\theta = \theta_0(r) + \vartheta$ , where  $\theta_0$  is the solution of Eq. (5), describing a static vortex structure, and  $\mu = (\vec{l} \cdot \vec{e}_2)$  is the azimuthal component of  $\vec{l}$ . In linear approximation, the equations for  $\vartheta$  and  $\mu$  become a set of coupled partial differential equations,

$$\begin{aligned} \left[ \nabla_x^2 - V_1(x) - \hat{H}_1 \right] \vartheta + \frac{2 \cos \theta_0}{x^2} \frac{\partial \mu}{\partial \chi} &= \frac{l_0^2}{c^2} \frac{\partial^2 \vartheta}{\partial t^2}, \\ \left[ \nabla_x^2 - V_2(x) - \hat{H}_2 \right] \mu - \frac{2 \cos \theta_0}{x^2} \frac{\partial \vartheta}{\partial \chi} &= \frac{l_0^2}{c^2} \frac{\partial^2 \mu}{\partial t^2}, \end{aligned} \quad (10)$$

where  $x = r/l_0$ ,  $\theta_0 = \theta_0(x)$  is the solution of Eq. (5), and  $\nabla_x = l_0 \nabla$ . The equations are symmetric in  $\vartheta$  and  $\mu$  with local Schrödinger-type differential operators in front, as well as with non-local parts  $\hat{H}_1$ ,  $\hat{H}_2$ . The ‘‘potentials’’  $V_1$ ,  $V_2$  in local Schrödinger-type operators are determined by  $W_0[\vec{l}]$ , see Eq. (3); they have the same form as for easy-plane magnets,<sup>41,43</sup>

$$V_1 = \left( \frac{1}{x^2} - 1 \right) \cos 2\theta_0, \quad V_2 = \left( \frac{1}{x^2} - 1 \right) \cos^2 \theta_0 - \left( \frac{d\theta_0}{dx} \right)^2. \quad (11)$$

Note that the potentials in this Schrödinger-type operators are not small, but localized near the vortex core. Non-local magnetostatic effects, defined by magnetic dipole interactions, are included in the integral operators,  $\hat{H}_1$ ,  $\hat{H}_2$ . For a ferromagnetic vortex, their form was determined and their role was discussed in Refs. 26,36. Generally, for antiferromagnets the magnetization includes not only terms proportional to the in-plane components of  $\vec{l}$ , but also time derivatives of the vector  $\vec{l}$ . For this reason, the structure of these operators presented though the vector  $\vec{l}$  is much more complicated than the corresponding structure for ferromagnets. But the non-local contributions to (10) are essential only for in-plane modes with low frequencies  $\omega \ll \gamma H_{DM}$ , and for this case the dynamical part of the magnetization is negligible, as shown below. By means of this approximation, one can demonstrate that the operators  $\hat{H}_{1,2}$ , corresponding to volume and to edge magnetic charges, take the same form as for a ferromagnetic vortex, after replacing  $M_s \rightarrow M_{DM}$  and  $M_z \rightarrow 0$ . In particular, the angular dependence of the eigenfunctions for these operators is the same as for ferromagnetic vortices, namely,  $\hat{H}_{1,2} \exp(im\chi) = \Lambda_{|m|} \exp(im\chi)$ , where the integer  $m$  ( $m = 0, \pm 1, \pm 2, \dots$ ) is the azimuthal number. Thus for AFM vortices, even considering the non-local magnetic

dipole interaction with  $\vec{M} \propto (\vec{l} \times \vec{d})$ , the separation of the radial and azimuthal parts of the deviations is possible, and the magnon modes are of the form  $\exp(im\chi)f_m(r)$ . This property is of importance for the problem of magnon modes above the AFM vortex ground state.

Thus, the static part of the equations (10), both local and non-local terms, have the same form as for the well-studied case of the ferromagnetic vortex, but the dynamical parts differ strongly. This produces a crucial difference in the magnon modes of these magnets. For ferromagnetic vortices, the magnon eigenstates  $\{\vartheta_m, \mu_m\}$  depend on  $\chi$  and  $t$  in combinations as  $\sin(m\chi + \omega t)$  or  $\cos(m\chi + \omega t)$ , whereas for a AFM vortex, a more general ansatz of the form

$$\begin{aligned}\vartheta_\alpha &= f_\alpha(r)(Ae^{im\chi} + Be^{-im\chi})\exp(i\omega_\alpha t) + \text{c.c.} \\ \mu_\alpha &= ig_\alpha(r)(Ae^{im\chi} - Be^{-im\chi})\exp(i\omega_\alpha t) + \text{c.c.}\end{aligned}\tag{12}$$

is appropriate.<sup>43</sup> Here  $\alpha = (n, m)$  is a full set of discrete numbers labelling the magnon eigenstates, and  $n$  is the nodal number. Substitution of this ansatz demonstrates, in contrast to the case of a ferromagnetic vortex, the full degeneracy of the frequency over the sign of  $m$ .<sup>43</sup> As a change of sign in the number  $m$  can also be interpreted as a change of the sense of rotation of the eigenmode (change of sign in the eigenfrequency  $\omega$ ), physically we have the situation of two independent oscillators rotating clock- and counter-clockwise with the same frequency (which can also be combined to give two linear oscillators in independent directions). This degeneracy was clearly demonstrated by solving the ordinary differential equations for  $f_\alpha$  and  $g_\alpha$  (10), as well as due to direct numerical simulations of the magnon modes above an AFM vortex.<sup>43</sup> Thus, the absence of gyroscopical properties for the  $\sigma$ -model equation is manifested in the fact that for a AFM vortex the modes with azimuthal numbers  $m = |m|$   $m = -|m|$  are degenerate, i.e., the splitting of doublets with  $m = \pm|m|$ , typical for the ferromagnetic vortex, is completely absent.<sup>43,44</sup>

Note one more important difference from the ferromagnetic case: for the AFM vortex the coupling of in-plane and out-of-plane oscillations comes only from the term with  $(\cos\theta_0)(\partial/\partial\chi)$ . This means, that (i) for any mode the coupling vanishes exponentially at  $x \rightarrow \infty$ ; (ii) the modes of radially symmetric ( $m = 0$ ) in-plane and out-of-plane oscillations are completely uncoupled. Both properties will be employed below for calculating of the magnon frequencies.

## B. Collective variables for vortex core oscillations.

First note that the equation (10) for an infinite magnet has a simple zero-frequency solution with  $m = 1$

$$\vartheta = (\vec{a} \cdot \nabla \theta_0), \quad \mu = \sin \theta_0 (\vec{a} \cdot \nabla \phi_0),$$

where  $\vec{a}$  is an arbitrary vector, and  $\theta_0, \phi_0$  describe the static vortex solution. Indeed, this perturbation describes a displacement of the vortex for a (small) vector  $\vec{a}$ . Such “zero mode” appears for any soliton problem, reflecting an arbitrary choice of the soliton (vortex) position.<sup>4</sup> For finite-size magnets, such modes beget low-frequency modes corresponding to the motion of a vortex core. Their analysis with the equations (10) is quite complicated, but it can be done within the approach based on the scattering amplitude formalism, which is developed for the Gross-Pitaevski equation<sup>6</sup> and local models for easy plane magnets.<sup>41</sup> But there is an easier and more convenient way to calculate the frequency of this mode based on a collective variable approach. Here the collective-variable is the vortex coordinate  $\vec{X}$ , which motion is described by a characteristic dynamic equation.<sup>38,41</sup>

Thus, for an AFM vortex, as well as for ferromagnets, one can expect the appearance of a special mode of vortex core oscillations. But the dynamical equations for the AFM vortex core coordinate differ significantly from that for ferromagnets. The  $\sigma$ -model equation contains a dynamical term with a second time derivative of  $\vec{l}$ , combined with gradients of  $\vec{l}$  in the Lorentz-invariant form  $d^2\vec{l}/dt^2 - c^2\nabla^2\vec{l}$ , whereas the Landau–Lifshitz equation is first-order in time. The chosen speed  $c = \gamma\sqrt{AH_{\text{ex}}/M_0}$  plays roles of both the magnon speed and the speed limit of solitons, it is only determined by the exchange interaction and attains tens km/s; e.g.,  $c \simeq 1.4 \cdot 10^4$  m/s for iron borate and  $c \simeq 2 \cdot 10^4$  m/s for orthoferrites.<sup>7</sup>

The formal Lorentz-invariance of spin dynamics of antiferromagnets manifests itself in the motion of any AFM solitons,<sup>45</sup> in particular, the motion of the AFM vortex core:<sup>42,46</sup> the dynamical equation for the core coordinate at small vortex speed  $\vec{X}$ , when at  $|d\vec{X}/dt| \ll c$ , possess an inertial term,

$$M_v \frac{d^2\vec{X}}{dt^2} = \vec{F},$$

where the effective vortex mass  $M_v = E_v/c^2$ , and  $\vec{F}$  is an external force acting on vortex. For the case of interest here, the free dynamics of the vortex in a circular sample,  $\vec{F}$  is the restoring force: in linear approximation  $\vec{F} = -\kappa\vec{X}$ , where  $\kappa$  is the stiffness coefficient. With this force, the vortex core dynamics is not a precession, as for the gyroscopic Thiele

equation for ferromagnetic vortices,<sup>47-49</sup> but rectilinear oscillations,  $\vec{X}(t) = \vec{a} \cos(\omega_v t + \phi_0)$ , degenerate with respect to the direction  $\vec{a}$  and  $\phi_0$ , with frequency  $\omega_v = \sqrt{\kappa/M_v}$ . For the easy-plane AFM model with  $W_m = 0$ , such dynamics has been observed by direct numerical simulations.<sup>27,44</sup> For a vortex state dot with  $R > R_{\text{crit}}$ , the value of  $\kappa$  is determined by the demagnetizing field, its value can be obtained from the known value for a ferromagnet by replacing  $M_s \rightarrow M_{\text{DM}}$ ,<sup>38</sup> which gives  $\kappa = 10 \cdot 4\pi M_{\text{DM}}^2 L^2 / 9R$ , and

$$\omega_v = \frac{2cM_{\text{DM}}\sqrt{10L}}{3\sqrt{AR \ln(\rho R/l_0)}}. \quad (13)$$

A simple estimate gives that  $\omega_v$ , as for a ferromagnetic vortex, is in the subGHz region, but with different (approximately square root, instead of linear for ferromagnetic vortex) dependence on the aspect ratio  $L/R$ .

### C. Other low-frequency modes.

Far from the vortex core, the other modes from this set are approximately characterized by in-plane oscillations of  $\vec{l}$  and  $\vec{M}$ . As their frequencies are small,  $\omega \ll \gamma H_{\text{DM}}$ , for these modes the magnetization  $\vec{M}$  is determined mainly by the in-plane static contribution (1), and the formulae for the demagnetization field energy for ferromagnetic vortices can be used. Moreover, the data known for the ferromagnetic magnon frequencies  $\omega_m^{\text{FM}}$  (in first approximation over the small parameter  $L/R$ , i.e., in the magnetostatic approximation), can be directly used for the calculation of the corresponding frequencies for magnon modes above the AFM vortex ground state. Note that, in this approximation,  $\omega_{+m}^{\text{FM}} = \omega_{-m}^{\text{FM}} = \omega_m^{\text{FM}}$ , because the doublet splitting for a ferromagnetic vortex is proportional to  $(L/R)^2$ ; see Refs. 26,40.

To make this essential simplification, note that for the ferromagnetic case the Landau-Lifshitz equation, linearized over the vortex ground state, can be written as  $\partial m_r / \partial t = 4\pi\gamma M_s m_z$ ,  $\partial m_z / \partial t = \hat{h}_2 M_s m_r$ , as was shown in Appendix B of Ref. 36. Here the dimensionless operator  $\hat{h}_2$  determines the non-local magnetostatic part of the magnetic dipole interaction. Then the equations can be easily rewritten as  $\partial^2 m_r / \partial t^2 + (\omega_m^{\text{FM}})^2 m_r = 0$ , where  $\omega_m^{\text{FM}} = 4\pi\gamma M_s \sqrt{\langle \hat{h}_2 \rangle}$ , where  $\langle \hat{h}_2 \rangle$  is the eigenvalue of the operator  $\hat{h}_2$ . These values for modes with different angular dependence can be either estimated theoretically or taken from experiments.<sup>36</sup>

Now we will return to the case of AFM vortices. Neglecting the vortex core contribution,

the second equation of the system (10) reduces to the form

$$\partial^2 \mu / \partial t^2 = (c/l_0)^2 \hat{H}_2 \mu,$$

having exactly the same structure as the equation for  $m_r$  for a ferromagnetic vortex. For the simplified form of the magnetization,  $\vec{M} = M_{\text{DM}}(\vec{l} \times \vec{e}_z)$  the same “magnetic charges”, both volume charges,  $\text{div} \vec{M}$ , and surface charges,  $(\vec{e}_r \cdot \vec{M})$ , as for a ferromagnetic vortex, are produced. Thus the operator  $\hat{h}_2$  differs from  $\hat{H}_2$  by a simple scaling relation,  $M_s \rightarrow M_{\text{DM}}$  and  $A/4\pi M_s^2 \rightarrow l_0^2$ , which gives  $\hat{H}_2 = (4\pi M_{\text{DM}}^2/K)\hat{h}_2$ . Then, it is easy to obtain the frequency of the AFM mode  $\omega_m$  in terms of the frequency of the ferromagnetic mode  $\omega_m^{\text{FM}}$  (if it is known) as follows

$$\omega_m = \frac{cM_{\text{DM}}}{\gamma M_s \sqrt{4\pi A}} \cdot \omega_m^{\text{FM}}. \quad (14)$$

In particular, the frequency of radially symmetric oscillations, having the highest frequency<sup>36</sup> for modes with minimal nodal number  $n$ , can be presented through the known value for  $\omega_0^{\text{FM}}$  as<sup>50</sup>

$$\omega_0 = \frac{2cM_{\text{DM}}\sqrt{L}}{\sqrt{AR}} \sqrt{\ln\left(\frac{6R}{L}\right)}. \quad (15)$$

For these modes, the frequencies are of the order of a few of GHz, with an approximately square root dependence on the aspect ratio  $L/R$ .

Note the absence of gyroscopic properties for the  $\sigma$ -model equation. This is manifested both in the absence of a gyroforce for an AFM vortex, as well as in the fact that for an AFM vortex the modes with the azimuthal numbers  $m = |m|$   $m = -|m|$  are degenerate. The splitting of doublets with  $m = \pm|m|$ , typical for ferromagnetic vortices, is absent for AFM vortices.<sup>43,44</sup>

#### D. Out of plane high-frequency modes.

For an AFM sample in the vortex state, the high-frequency QAF branch of magnons begets a set of discrete modes with frequencies of the order of  $\omega_g$ , i.e. hundreds of GHz. For all these modes far from the vortex core, oscillations of the vector  $\vec{l}$  are out of plane, and the static contribution to the weak magnetization,  $\vec{m}_{\text{static}} \propto (\vec{e}_z \times \vec{l})$  is absent, see (1). Moreover, it is easy to show that the dynamical part of  $\vec{m}$ ,  $\vec{m}_{\text{dyn}} \propto (\vec{l} \times \partial \vec{l} / \partial t)$  has a vortex-like structure and does not lead to magnetic poles neither on the up and down surfaces nor at the edge.

Hence, the dipole interaction is not essential for the description of high-frequency magnons, and the results obtained earlier for the vortex in easy-plane antiferromagnets without the magnetic dipole interaction<sup>43,44</sup> can be used as a good approximation. In particular, the frequencies  $\omega_{n,m}$  are close to  $\omega_g$ , and the difference  $(\omega_{n,m} - \omega_g)$  decreases as the dot radius increases.

For an AFM vortex within the local easy-plane model, the set of high-frequency radially-symmetric modes with  $m = 0$  includes a *truly local* mode with an amplitude exponentially localized within an area of the order of  $5l_0$  and with a frequency  $\omega_1 \sim 0.95\omega_g$  independent on  $R$ . Note that the frequency of this mode is *inside* the range of low-frequency in-plane modes, and hence, we have an example of a truly local mode inside a continuum spectrum.

The presence of a local mode inside the frequency region of low-frequency modes is quite a delicate feature, and it is interesting to discuss whether or not such mode survives for the vortex state AFM dots when accounting for dipole interactions. It is easy to show that for these modes the oscillations of  $\vec{l}$  have no in-plane component, only the  $\vartheta \neq 0$ , even inside the core region. Thus, for this mode the oscillations of  $\vec{m}$  are such that they do not disturb the vortex-like closed-flux structure

$$\delta\vec{m} \propto \vec{e}_\chi [(\partial\vartheta/\partial t) + \gamma H_D \vartheta \cos \theta_0],$$

and all the magnetic poles vanish exactly. Hence, for cylindrical dots made with canted antiferromagnets in the vortex state, a radially symmetric mode with exponential localization inside an area of radius 30–40 nm near the vortex core appears. The frequency of this mode is approximately 5% below the energy gap of out-of-plane modes  $\omega_g$ , which gives  $\sim 9$  GHz for hematite and  $\sim 15$  GHz for iron borate. We now stress that such modes are absent for ferromagnetic vortices. This mode can be imaged as an oscillation of the vortex core size, with keeping the in-plane vortex-like structure for  $\vec{m}$ . The total magnetic moment connected to this oscillations is zero, and the excitation of these oscillations by a uniform magnetic field, either pulsed or periodic, is impossible. However, such oscillations can be excited by an instant change of the uniaxial anisotropy, which determines the vortex core size. The novel technique<sup>18–21</sup> of spin excitations by ultra-short laser pulses can be applied here, because the linearly polarized light at inclined incidence, due to an ultra-fast inverse Cotton-Mouton or inverse Voigt effect, is equivalent to the necessary change of uniaxial anisotropy.



## V. CONCLUSION.

To conclude, for micron-sized samples of typical canted antiferromagnets, their ground state exhibits a topologically non-trivial spin distribution. The magnetizations of each sublattice  $\vec{M}_1$  and  $\vec{M}_2$  are characterized by a vortex state with a standard out-of-plane structure, but the net magnetization  $\vec{M} = \vec{M}_1 + \vec{M}_2$  forms a planar vortex, where the projection of the magnetization normal to the vortex plane everywhere in the sample is zero; in particular,  $\vec{M} = 0$  in the vortex center. The vortex state AFM dots possess a rich variety of normal magnon modes, from rectilinear oscillations of the vortex core position with sub-GHz frequency to out-of-plane modes with frequencies of the order of hundreds of GHz, including a truly local mode. The use of QAF modes for vortex state AFM dots, particularly the truly local mode, would allow the application of magnonics for higher frequencies until  $\sim 0.3$  THz. This mode can be excited by ultra-short laser pulses with linearly polarized light.

Our theory would be applicable to other systems with an AFM spin structure, like a ferromagnetic bilayer dot containing two thin ferromagnetic films with an AFM interaction between them, described by the field  $H_{\text{ex}}$ . If  $H_{\text{ex}}$  is large enough,  $H_{\text{ex}} > 4\pi M_s$ , the anti-phase oscillations of the magnetic moments of the layers produce high-frequency modes with frequencies of the order of  $\sqrt{\gamma H_{\text{ex}} \omega_{m,n}^{\text{FM}}}$ , where  $\omega_{m,n}^{\text{FM}}$  are the frequencies of the modes for a single layer dot.

### Acknowledgments

We gratefully acknowledge partial support from the National Security Agency, Laboratory of Physical Sciences, Army Research Office, National Science Foundation grant No. 0726909, and JSPS-RFBR contract No. 09-02-92114. E.G. and B.I. acknowledge partial support from a joint grant from the Russian Foundation for Basic Research and Ukraine Academy of Science, and from Ukraine Academy of Science via Grant No. VC 38/ V 139-18.

---

\* Electronic address: bivanov@i.com.ua

<sup>1</sup> R. Skomski, J. Phys.: Condens. Matter **15**, R841 (2003); Advanced Magnetic Nanostructures, edited by D. J. Sellmyer and R. Skomski (Springer, Berlin, 2006).

- <sup>2</sup> R. Hertel, W. Wulfhchel, and J. Kirschner, Phys. Rev Lett. **93**, 257202 (2004).
- <sup>3</sup> G. E. Volovik, *The Universe in a Helium Droplet* (Clarendon, Oxford, 2003)
- <sup>4</sup> N. Manton and P. Sutcliffe, *Topological Solitons* (Cambridge University Press, Cambridge, 2004).
- <sup>5</sup> P. G. de Gennes, *Superconductivity of Metals and Alloys* (W. A. Benjamin, New York, 1966).
- <sup>6</sup> L. Pitaevskii, and S. Stringari, *Bose-Einstein Condensation* (Clarendon, Oxford, 2003).
- <sup>7</sup> V. G. Baryakhtar, B. A. Ivanov and M. V. Chetkin, Sov. Phys. Usp. **28**, 563 (1985); V. G. Bar'yakhtar, M. V. Chetkin, B. A. Ivanov and S. N. Gadetskii, *Dynamics of topological magnetic solitons. Experiment and theory*, Springer Tract in Modern Physics **139** (Springer-Verlag, Berlin, 1994).
- <sup>8</sup> A. M. Kosevich, B. A. Ivanov, and A. S. Kovalev, Phys. Reports **194**, 118 (1990).
- <sup>9</sup> V. G. Bar'yakhtar and B. A. Ivanov, *Solitons and Thermodynamics of Low-Dimensional Magnets*, in: *Soviet Scientific Reviews, Section A. Physics*, I. M. Khalatnikov (ed.), **16**, 1 (1992).
- <sup>10</sup> B. A. Ivanov and A. K. Kolezhuk, Phys. Rev. B **68**, 052401 (2003).
- <sup>11</sup> B. A. Ivanov, JETP Lett. **84**, 84 (2006); B. A. Ivanov, R. S. Khymyn and A. K. Kolezhuk, Phys. Rev. Lett. **100**, 047203 (2008).
- <sup>12</sup> D. D. Wiesler, H. Zabel, and S. M. Shapiro, Z. Phys. B **93**, 277 (1994).
- <sup>13</sup> F. G. Mertens and A. R. Bishop, in *Nonlinear Science at the Dawn of the 21th Century*, edited by P. L. Christiansen and M. P. Soerensen (Springer, Berlin, 2000).
- <sup>14</sup> D. A. Dimitrov and G. M. Wysin, Phys. Rev. B **50**, 3077 (1994); *ibid.* **51**, 11947 (1995).
- <sup>15</sup> V. E. Kireev, B. A. Ivanov, Phys. Rev. B. **68**, 104428 (2003); O. Tchernyshyov, G.-W. Chern, Phys. Rev. Lett. **95**, 197204 (2005).
- <sup>16</sup> R. Antos, Y. Otani, and J. Shibata, J. Phys. Soc. Jpn. **77**, 031004 (2008).
- <sup>17</sup> K. Yu. Guslienko, J. Nanosci. Nanotechnol. **8**, 2745 (2008).
- <sup>18</sup> A. V. Kimel, A. Kirilyuk, A. Tsvetkov, R. V. Pisarev, and Th. Rasing, Nature **429**, 850 (2004); A. V. Kimel, A. Kirilyuk, P. A. Usachev, R. V. Pisarev, A. M. Balbashov, and Th. Rasing, Nature **435**, 655 (2005).
- <sup>19</sup> A. V. Kimel, B. A. Ivanov, R. V. Pisarev, P. A. Usachev, A. Kirilyuk, and Th. Rasing, Nat. Phys. **5**, 727 (2009).
- <sup>20</sup> A. M. Kalashnikova, A. V. Kimel, R. V. Pisarev, V. N. Gridnev, A. Kirilyuk, and Th. Rasing, Phys. Rev. Lett. **99**, 167205 (2007); A. M. Kalashnikova, A. V. Kimel, R. V. Pisarev, V. N.

- Gridnev, P. A. Usachev, A. Kirilyuk, and Th. Rasing, Phys. Rev. B **78**, 104301 (2008).
- <sup>21</sup> T. Satoh, S.-J. Cho, R. Iida, T. Shimura, K. Kuroda, H. Ueda, Y. Ueda, B. A. Ivanov, F. Nori, and M. Fiebig, arXiv:1003.0820 (unpublished).
- <sup>22</sup> A. Hubert and R. Schafer, *Magnetic Domains* (Springer, Berlin, 1998).
- <sup>23</sup> B. A. Ivanov and E. V. Tartakovskaya, Phys. Rev. Lett. **77**, 386 (1996).
- <sup>24</sup> A. I. Akhiezer, V. G. Bar'yakhtar, and S. V. Peletminskii, *Spin Waves* (North-Holland, Amsterdam, 1968).
- <sup>25</sup> B. A. Ivanov and C. E. Zaspel, Appl. Phys. Lett. **81**, 1261 (2002).
- <sup>26</sup> B. A. Ivanov and C. E. Zaspel, Phys. Rev. Lett. **94**, 027205 (2005).
- <sup>27</sup> A. R. Völkel, F. G. Mertens, A. R. Bishop, and G. M. Wysin, Phys. Rev. B **43**, 5992 (1991).
- <sup>28</sup> C. A. Ross, M. Hwang, M. Shima, J. Y. Cheng, M. Farhoud, T. A. Savas, H. I. Smith, W. Schwarzacher, F. M. Ross, M. Redjald, and F. B. Humphrey, Phys. Rev. B **65**, 144417 (2002).
- <sup>29</sup> N. A. Usov, S. E. Peschany, Fiz. Met. Metalloved. **78**, 13 (1994), [In Russian].
- <sup>30</sup> R. Höllinger, A. Killinger, U. Krey, J. Magn. Magn. Mater. **261**, 178 (2003).
- <sup>31</sup> K. Yu. Guslienko and V. Novosad, J. Appl. Phys. **96**, 4451 (2004).
- <sup>32</sup> V. P. Kravchuk and D. D. Sheka, Physics of the Solid State, **49**, 1923 (2007).
- <sup>33</sup> Wijn, H. P. J. (ed.) *Numerical Data and Functional Relationships*, Landolt-Börnstein, New Series, Group III, **27** (Springer, Berlin, 1981).
- <sup>34</sup> L. Giovannini, F. Montoncello, F. Nizzoli, G. Gubbiotti, G. Carlotti, T. Okuno, T. Shinjo, and M. Grimsditch, Phys. Rev. B **70**, 172404 (2004).
- <sup>35</sup> M. Buess, R. Höllinger, T. Haug, K. Perzlmaier, U. Krey, D. Pescia, M. R. Scheinfein, D. Weiss, and C. H. Back, Phys. Rev. Lett. **93**, 077207 (2004)
- <sup>36</sup> M. Buess, T. P. J. Knowles, R. Höllinger, T. Haug, U. Krey, D. Weiss, D. Pescia, M. R. Scheinfein, and C. H. Back, Phys. Rev. B **71**, 104415 (2005).
- <sup>37</sup> C. E. Zaspel, B. A. Ivanov, P. A. Crowell and J. Park, Phys. Rev. B **72**, 024427 (2005).
- <sup>38</sup> K. Yu. Guslienko, B. A. Ivanov, Y. Otani, H. Shima, V. Novosad, and K. Fukamichi, J. Appl. Phys. **91**, 8037 (2002).
- <sup>39</sup> K. Yu. Guslienko, W. Scholz, R. W. Chantrell, and V. Novosad, Phys. Rev. B **71**, 144407 (2005).
- <sup>40</sup> K. Y. Guslienko, A. N. Slavin, V. Tiberkevich, and S.-K. Kim, Phys. Rev. Lett. **101**, 247203 (2008).
- <sup>41</sup> B. A. Ivanov, H. Schnitzer, F. G. Mertens, and G. M. Wysin, Phys. Rev. B **58**, 8464 (1998).

- <sup>42</sup> G. M. Wysin, Phys. Rev. B **54**, 15156 (1996).
- <sup>43</sup> B. A. Ivanov, A. K. Kolezhuk, and G. M. Wysin, Phys. Rev. Lett. **76**, 511 (1996).
- <sup>44</sup> G. M. Wysin and A. R. Völkel, Phys. Rev. B **54**, 12921 (1996).
- <sup>45</sup> I. V. Bar'yakhtar and B. A. Ivanov, Sol. St. Commun. **34**, 545 (1980); Sov. Phys.– JETP **85**, 328 (1983).
- <sup>46</sup> B. A. Ivanov and D. D. Sheka, Phys. Rev. Lett. **72**, 404 (1994).
- <sup>47</sup> A. A. Thiele, Phys. Rev. Lett. **30**, 239 (1973).
- <sup>48</sup> D. L. Huber, Phys. Rev. B **26**, 3758 (1982).
- <sup>49</sup> A. V. Nikiforov and É. B. Sonin, Sov. Phys. JETP **58**, 373 (1983).
- <sup>50</sup> C. E. Zaspel, E. S. Wright, A. Yu. Galkin, and B. A. Ivanov, Phys. Rev. B **80**, 094415 (2009).